



The lesion characteristics assessed by LGE-MRI after the cryoballoon ablation and conventional radiofrequency ablation

Kurose, Jun ; Kiuchi, Kunihiro ; Fukuzawa, Koji ; Mori, Shumpei ;
Ichibori, Hiroto ; Konishi, Hiroki ; Taniguchi, Yayoi ; Hyogo, ...

(Citation)

Journal of Arrhythmia, 34(2):158-166

(Issue Date)

2018-04

(Resource Type)

journal article

(Version)

Version of Record

(Rights)

© 2018 The Authors. Journal of Arrhythmia published by John Wiley & Sons Australia, Ltd on behalf of the Japanese Heart Rhythm Society.
This is an open access article under the terms of the Creative Commons Attribution-NonCommercial License, which permits use, distribution and reproduction in any medium...

(URL)

<https://hdl.handle.net/20.500.14094/90004853>



The lesion characteristics assessed by LGE-MRI after the cryoballoon ablation and conventional radiofrequency ablation

Jun Kurose MD¹ | Kunihiro Kiuchi MD, FHR¹  | Koji Fukuzawa MD¹ |
Shumpei Mori MD² | Hirotoshi Ichibori MD¹ | Hiroki Konishi MD¹ | Yayoi Taniguchi
MD¹ | Kiyohiro Hyogo MD¹ | Hiroshi Imada MD¹  | Hideya Suehiro MD¹ |
Yu-ichi Nagamatsu MD¹ | Tomomi Akita MD¹ | Makoto Takemoto MD¹ |
Ken-ichi Hirata MD² | Shinsuke Shimoyama MD³ | Yoshiaki Watanabe MD³ |
Tatsuya Nishii MD³ | Noriyuki Negi RT⁴ | Katsusuke Kyotani RT⁴

¹Section of Arrhythmia, Division of Cardiovascular Medicine, Department of Internal Medicine, Kobe University Graduate School of Medicine, Chuo-ku, Kobe city, Japan

²Division of Cardiovascular Medicine, Department of Internal Medicine, Kobe University Graduate School of Medicine, Chuo-ku, Kobe city, Japan

³Department of Radiology, Kobe University Graduate School of Medicine, Chuo-ku, Kobe city, Japan

⁴Division of Radiology, Center for Radiology and Radiation Oncology, Kobe University Hospital, Chuo-ku, Kobe city, Japan

Correspondence

Kunihiro Kiuchi, Division of Cardiovascular Medicine, Department of Internal Medicine, Kobe University Hospital, Chuo-ku, Kobe city, Japan.
Email: kunihiokiuchi@yahoo.co.jp

Abstract

Background: Rhythm outcomes after the pulmonary vein isolation (PVI) using the cryoballoon (CB) are reported to be excellent. However, the lesions after CB ablation have not been well discussed. We sought to characterize and compare the lesion formation after CB ablation with that after radiofrequency (RF) ablation.

Methods: A total of 42 consecutive patients who underwent PVI were enrolled (29 in the CB group and 13 in the RF group). The PVI lesions were assessed by late gadolinium enhancement magnetic resonance imaging 1–3 months after the PVI. The region around the PVs was divided into eight segments: roof, anterior-superior, anterior-carina, anterior-inferior, bottom, posterior-inferior, posterior-carina, and posterior-superior segment. The lesion width and lesion gap in each segment were compared between the two groups. Lesion gaps were defined as no-enhancement sites of >4 mm.

Results: As compared to the RF group, the overall lesion width was significantly wider and lesion gaps significantly fewer at the anterior-superior segment of the left PV (LAS) and anterior-inferior segment of the right PV (RAI) in the CB group (lesion width: 8.2 ± 2.2 mm vs 5.6 ± 2.0 mm, $P = .001$; lesion gap at LAS: 7% vs 38%, $P = .02$; lesion gap at RAI: 7% vs 46%, $P = .006$).

Conclusions: The PVI lesions after CB ablation were characterized by extremely wider and more continuous lesions than those after RF ablation.

KEYWORDS

atrial fibrillation, cryoballoon ablation, late gadolinium enhancement MRI, pulmonary vein isolation, radiofrequency ablation

1 | INTRODUCTION

Late gadolinium enhancement (LGE) magnetic resonance imaging (MRI) is reported to detect fibrosis of the myocardium. The absence of a LGE in the left ventricle could predict a low potential risk of sudden cardiac death and life-threatening ventricular events.¹ Recently, the distribution of the fibrosis in the left atrium could be associated with a recurrence after atrial fibrillation (AF) ablation.^{2–4} Furthermore, the lesions after AF ablation using conventional ablation catheters with radiofrequency (RF) energy could be visualized by LGE-MRI, and the lesion gaps could be associated with electrical reconduction sites in the 2nd procedure.^{5,6} Although the lesions after AF ablation using cryoballoon (CB) catheters are likely wide and homogeneous, the lesions have not been well characterized.⁷ It is still in debate whether the lesion formation could differ between the different energy sources.^{8,9} Therefore, we sought to visualize and characterize the lesions created by CB ablation and conventional AF ablation with RF energy using LGE-MRI. Furthermore, we measured and compared the creatinine kinase (CK) as a biomarker of myocardial injury with the different ablation procedures.

2 | METHODS

2.1 | Patients

A total of 51 consecutive patients who underwent pulmonary vein isolation (PVI) were enrolled in this study. Of them, 34 (67%) of 51 patients underwent cryoballoon (CB) ablation (CB group) and the remaining 17 underwent radiofrequency (RF) ablation (RF group). Five patients in the CB group and 4 in the RF group were excluded from this study because of a suboptimal imaging quality. The remaining 29 patients in the CB group and 13 in the RF group were enrolled in this study. The protocol for this research project has been approved by a suitably constituted Ethics Committee of the institution, and it conforms to the provisions of the Declaration of Helsinki. Committee of 2017.3.9., Approval No. 160014. All informed consent was obtained from the subject(s) and/or guardian(s).

2.2 | Mapping and ablation procedure

Prior to the procedure, transesophageal echocardiography was performed to exclude any thrombus formation. The patients were studied under deep propofol sedation while breathing spontaneously. Standard electrode catheters were placed in the right ventricular apex and coronary sinus after which a single transseptal puncture was performed. Unfractionated heparin was administered in a bolus form before the transseptal puncture to maintain an activated clotting time of >300 s. If AF occurred, internal electrical cardioversion was performed to restore sinus rhythm.

Mapping and ablation were performed using the CARTO3 system (Biosense Webster, Diamond Bar, CA, USA) or NavX system (St. Jude Medical, Inc., St. Paul, MI, USA) as a guide after integration of a three-dimensional (3D) model of the anatomy of the LA and PVs obtained

from pre-interventional computed tomography (CT) or magnetic resonance imaging (MRI). Prior to the ablation, the circular mapping catheter- (Lasso, Biosense Webster, Diamond Bar, Calif; Optima, St. Jude Medical Inc.) and ablation catheter-reconstructed LA posterior anatomies were aligned with the CT image or MRI.¹⁰

2.3 | Ablation procedure in the RF group

The RF alternating current was delivered in a unipolar mode between the irrigated tip electrode of the ablation catheter (Navistar Thermo-cool SmartTouch™, Biosense Webster; FlexAbility™, St. Jude Medical, Inc.) and an external back-plate electrode. The initial RF generator setting consisted of an upper catheter tip temperature of 43°C, maximal RF power of 30 W, and irrigation flow rate of 8 to 30 mL/min using the CARTO3 and NavX systems. In patients requiring RF applications to the posterior wall, the initial RF generator setting consisted of a maximal RF power of 20 W. All patients underwent an extensive encircling PVI. RF applications were performed in a "point-by-point" manner. The maximum time spent on the anterior and posterior walls was 30 and 20 s, respectively. The encircling ablation line was created approximately 0.5 to 1 cm from the PV ostia. The goal of each RF application was as follows: 1) the elimination of a negative component of the unipolar atrial electrogram and 2) the elimination of a positive deflection of the bipolar atrial electrogram during SR. If those findings could not be achieved after RF application, additional RF application at the same site was performed. The RF energy was routinely reduced by 10 W when ablating the posterior wall according to the esophageal temperature measured with an esophageal temperature probe (SensiTherm, St. Jude Medical). If the esophageal temperature rose to >39°C, the ablation was stopped immediately and the energy was further reduced. After the esophageal temperature decreased to the normal range (37°C), the RF application was resumed. If ablation could not be performed with 20 W, the line placement was performed either more antral or closer to the PV, depending on the individual's anatomical characteristics. Catheter navigation was performed with a steerable sheath (Agilis, St. Jude Medical Inc.).

2.4 | Ablation procedure in the CB group

A single transseptal puncture was performed. Complete occlusion was confirmed by injecting contrast medium. The PVI was performed with a second-generation cryoballoon (Arctic Front Advance, Medtronic, Minneapolis, MN, USA) with a freeze cycle of 180 s. If PV potentials remained, the operator decided whether additional CB ablation or touch-up RF ablation was applied.

The procedural endpoint was considered to be electrophysiologically proven bidirectional block of the PV-encircling ablation lines, which was confirmed with a circular mapping catheter in both the CB and RF groups. After proving bidirectional block of the PVs, we performed a stimulation protocol (burst pacing from CS with 300 ms, 250 ms, and 200 ms for 10s each) to test the inducibility. No adenosine infusion was performed to assess the dormant conduction in both RF and CB groups.

2.5 | MRI acquisition

All patients underwent contrast-enhanced MR imaging using a 1.5-T MR system (Achieva, Philips Medical, Best, The Netherlands) equipped with a 5-channel cardiac coil 1–3 months after the AF ablation. This scan technique has been established, and acquired images have been used for the AF ablation procedure.¹¹ First, contrast enhancement–magnetic resonance angiography (CE-MRA) of the PV–LA anatomy was acquired with a breath-hold 3D fast field echo (FFE) sequence in the coronal plane during the first pass of a contrast agent (gadobutrol, Gadovist; Bayer Yakuhin, Osaka, Japan) injection at a dose of 0.1 mmol/kg.^{11–13} Then, the LGE-MRI of the LA with PVs was acquired using a 3D inversion recovery, respiration-navigated, electrocardiogram-gated, T1-FFE sequence in the transverse plane 15 min after a contrast injection, which have been previously reported.¹⁴ The typical parameters were as follows: repetition time/echo time = 4.7 / 1.5 ms, voxel size = $1.43 \times 1.43 \times 2.40$ mm (reconstructed to $0.63 \times 0.63 \times 1.20$ mm), flip angle = 15, SENSE = 1.8, and 80 reference lines. The inversion time (TI) was set as 280 – 320 ms, using a Look-Locker scan. The data acquisition was performed during the mid-diastolic phase of the left ventricle. The typical scan time for the LGE-MRI study was 7 to 12 min depending on the patient's heart rate and respiration pattern. The images of the CE-MRA and LGE-MRI were transferred to a workstation (Ziostation ver. 2.4.2.3., Ziosoft Inc., Tokyo, Japan) for the further image postprocessing and image analysis.

2.6 | Three-dimensional visualization of Ablation lesions

The following image postprocessing was performed by the consensus of a board-certified diagnostic radiologist (T.N. with 10 years of experience) and a radiological technologist (N.N. with 10 years of

experience) unaware of the ablation methods. The three-dimensional (3D) visualization method for the LGE was as follows. First, the LA in LGE-MRI was segmented semi-manually by contouring the endocardial and epicardial borders of the atrium, including the PVs, while referring the CE-MRA. Second, the mean value and SD of the voxel intensity was measured on the “healthy” LA wall where no hyperenhanced areas in LGE-MRA were involved. Third, a voxel intensity histogram analysis of the LA wall identified the LGEs as intensities >2 SD on the “healthy” LA wall. Furthermore, the degree of intensity was categorized by color-coded scaling (green: >2 SD; yellow: 3–4SD; red: >4 SD). Finally, a 3D reconstruction, the color-coded LGE, and volume-rendered LA and PV image generated from CE-MRA were fused semi-automatically. According to the previous study, an ablation lesion was defined as an artificial LGE site with a signal intensity of >2 SD around the PV.^{11,12}

2.7 | Measurement of the ablation lesion

The region around the PV was divided into the following eight segments: roof, anterior-superior, anterior-carina, anterior-inferior, bottom, posterior-inferior, posterior-carina, and posterior-superior segments (Figure 1). The maximum width of the lesion and number and percentage of lesion gaps in each segment were calculated. Animal study reported that the maximum gap length with conduction block was 4 mm.¹⁵ According to their result, the lesion gaps were defined as no-enhancement sites of >4 mm.

2.8 | Measurement of creatine kinase

To assess the degree of the myocardial injury between the two different ablation procedures, the creatine kinase (CK) was measured one day before and after the AF ablation in all patients. If the

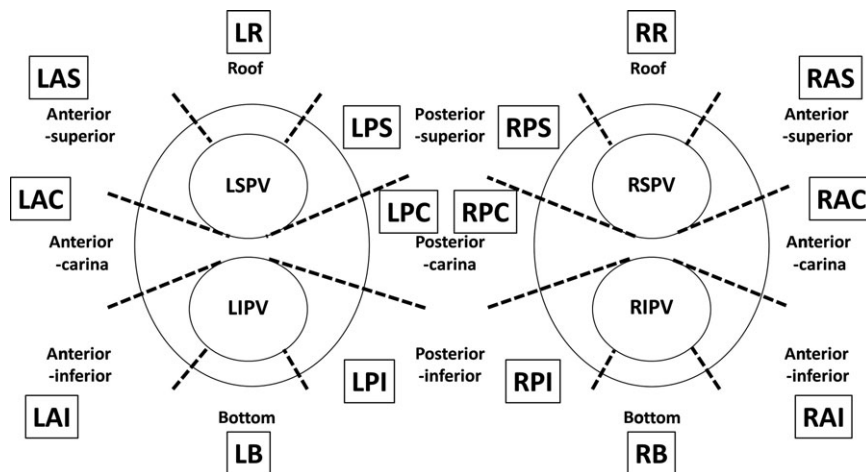


FIGURE 1 Segmentation of the ablation lesion around the pulmonary vein. LSPV, left superior pulmonary vein; LIPV, left inferior pulmonary vein; RSPV, right superior pulmonary vein; RIPV, right inferior pulmonary vein; LR, roof segment of the left PV; LAS, anterior-superior segment of the left PV; LAC, anterior-carina of the left PV; LAI, anterior-inferior segment of the left PV; LB, bottom segment of the left PV; LPI, posterior-inferior segment of the left PV; LPC, posterior-carina of the left PV; LPS, posterior-superior of the left PV; RR, roof segment of the right PV; RAS, anterior-superior segment of the right PV; RAC, anterior-carina of the right PV; RAI, anterior-inferior segment of the right PV; RB, bottom segment of the right PV; RPI, posterior-inferior segment of the right PV; RPC, posterior-carina of the right PV; RPS, posterior-superior of the right PV

baseline CK level was high or a CK elevation due to procedure-related complications or ischemic heart disease was present, the patients were excluded from this study.

2.9 | Statistical analysis

The data were tested with the Kolmogorov-Smirnov test. Continuous data were presented as the mean \pm SD for normally distributed variables. Medians and quartiles were given for non-normally distributed variables. If these data followed a normal distribution, they were tested with an unpaired *t* test or Welch test. When these data did not follow a normal distribution, they were tested with a Mann-Whitney test. In the comparison of the CK level before and after the AF ablation, they were tested with a paired *t* test. Categorical variables were analyzed with the chi-square test. A value of $P < .05$ was considered statistically significant. All statistical analyses were performed using SPSS, Release 24 software (SPSS, Chicago, IL, USA).

3 | RESULTS

3.1 | Patient characteristics

Nine patients (18%) were excluded from this study due to the poor MRI quality by consensus of 3 observers who were unaware of the ablation results. The possible reason of poor MRI quality was as follows: 1) unstable respiration, $n = 5$; 2) frequent ventricular premature beats, $n = 2$; and 3) inadequate MRI acquisition time from gadolinium injection, $n = 2$. The remaining 29 patients in the CB group and 13 in the RF group were enrolled in this study. The patient characteristics are displayed in Table 1. In the CB group, the patients with paroxysmal AF were more dominant and had a significantly lower CHADS₂ score, higher left atrial appendage (LAA) flow, shorter left atrial diameters (LAD), and lower BNP level than the RF group (PAF:26 [90%] of 29 vs 5 [38%] of 13 patients, $P = .001$; CHADS₂ score: 0.7 ± 0.8 vs 1.4 ± 1.0 , $P = .03$; LAA flow: 50 ± 20 vs 29 ± 16 mm/s, $P = .002$; LAD: 38 ± 5 vs 42 ± 4 mm, $P = .02$, BNP: 76 ± 74 vs 117 ± 60 pg/mL, $P = .018$). The procedure time was significantly shorter in CB group, but not the fluoroscopy time (procedure time: 171 ± 39 vs 233 ± 33 min, $P < .001$; fluoroscopy time: 53.4 ± 19.3 vs 58.5 ± 23.0 min, $P = .460$). Although transient phrenic nerve injury was observed in 1 (3.4%) of 29 CB group patients, no major adverse events were observed in both CB and RF groups. The days from the AF ablation to the MRI acquisition were comparable between the groups.

3.2 | Ablation lesion width assessed by LGE-MRI

Figure 2 shows the mean width of the ablation lesion in each segment. The ablation lesion was significantly wider in the CB group than in the RF group (8.2 ± 2.2 mm in CB group vs 5.6 ± 2.0 mm in RF group, $P = .001$). The mean width of the ablation lesion in

TABLE 1 Comparison of the patient characteristics between the CB and RF groups

	CB group N = 29	RF group N = 13	P-value
Age, year	64 ± 9	69 ± 7	.092
Male, n (%)	22 (76%)	11 (77%)	.633
AF type			
Paroxysmal, n (%)	26 (90%)	5 (38%)	.001
Persistent, n (%)	3 (10%)	9 (62%)	.001
Anti-arrhythmic drugs, n	0.9 ± 0.8	0.7 ± 0.8	.374
CHADS ₂ score, point	0.7 ± 0.8	1.4 ± 1.0	.030
LAA flow, cm/s	50 ± 20	29 ± 16	.002
LAD, mm	38 ± 5	42 ± 4	.020
LVEF, %	62 ± 5	60 ± 6	.305
BMI, kg/m ²	23 ± 2	24 ± 3	.317
BNP, pg/mL	76 ± 74	117 ± 60	.018
CK, IU/L	128 ± 66	126 ± 43	.707
eGFR, mL/min/1.73 m ²	67 ± 10	67 ± 11	.885
Procedure time, min	171 ± 39	233 ± 33	<.001
Fluoroscopy time, min	53 ± 19	59 ± 23	.460
Duration from ablation to MRI, day	44 ± 10	41 ± 10	.389

AF, atrial fibrillation; LAA, left atrial appendage; LAD, left atrial dimension; LVEF, left ventricular ejection fraction; BMI, body mass index; BNP, brain natriuretic peptide; CK, creatine kinase; eGFR, estimated glomerular filtration rate.

each segment was likely wider in the CB group, but not in the anterior-carina of the right PV (RAC) (lesion width on the RAC: 7.0 ± 3.1 mm in the CB group vs 7.4 ± 3.9 mm in the RF group, P value = .753). Of note, the lesion width at LAS, LAI, LPS, RR, RAS, RPI, RPC, and RPS was significantly wider in the CB group than in the RF group. Table 2 summarized the lesion width at each segment.

3.3 | Ablation lesion gap assessed by LGE-MRI

Figure 3 shows the percentage of the lesion gap at each segment. Lesion gaps were significantly fewer at the anterior-superior segment of the left PV (LAS) and anterior-inferior segment of the right PV (RAI) in the CB group as compared to the RF group (LAS: 2 [7%] of 29 in CB group vs 5 [38%] of 13 in RF group, $P = .021$; RAI: 2 [7%] of 29 in CB group vs 6 [46%] of 13 in RF group, $P = .006$). At the remaining 14 sites, the percentage of the lesion gap was comparative between the 2 groups. The segments with the highly documented lesion gap of $\geq 30\%$ were LR, LB, and RB in the CB group, while LR, LAS, LAI, LB, RPS, RB, and RAI in the RF group. Table 3 summarized the number and percentage of the lesion gap. In the subgroup without touch-up ablation, the segments where the lesion gap was highly documented were LR (7 (30%) of 23 patients) and LB (7 (30%) of 23 patients). Representative cases in both the CB and RF groups are shown in Figure 4.

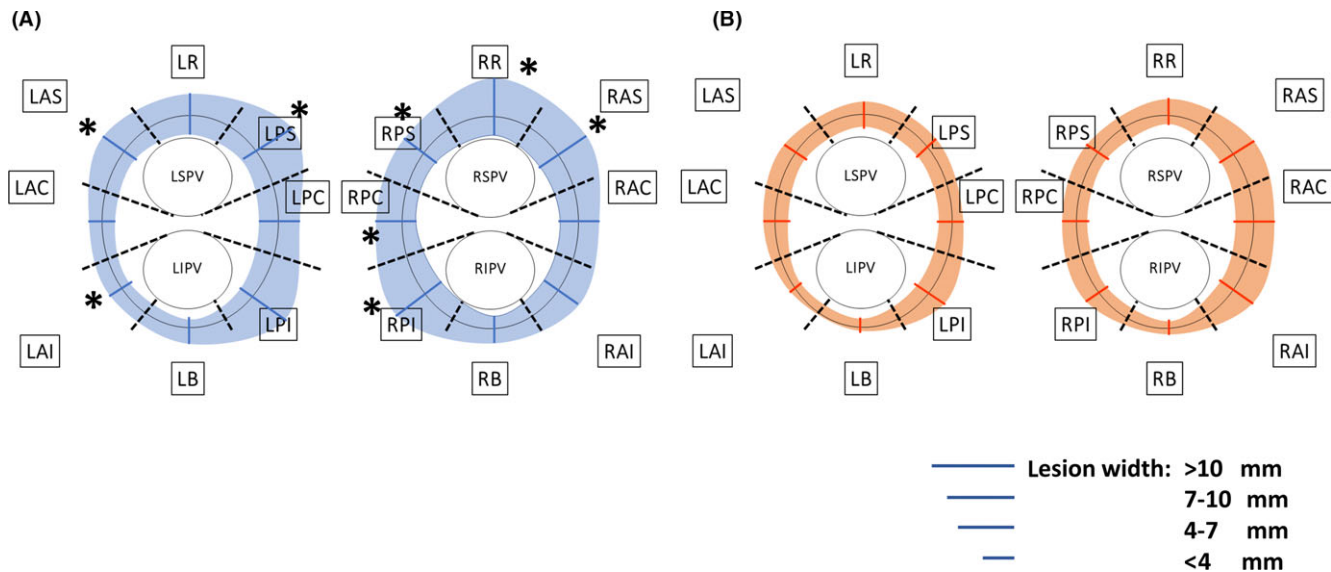


FIGURE 2 Comparison of the ablation lesion width between the CB and RF groups. A, Lesion width after CB ablation. B, Lesion width after RF ablation. The lesion width at LAS, LAI, LPS, RR, RAS, RPI, RPC, and RPS was significantly wider in the CB group compared to the RF group. Please see the detail value of the lesion width at the each segment in the text. *Significantly different at $P < .05$

TABLE 2 Ablation lesion width between the CB and RF groups

	CB group N = 29	RF group N = 13	P value
LR	7.1 ± 3.8	5.7 ± 4.6	.243
LAS	7.6 ± 3.8	4.1 ± 2.2	.020
LAC	4.6 ± 2.5	4.1 ± 2.1	.529
LAI	4.4 ± 1.9	2.7 ± 0.9	.023
LB	4.3 ± 1.9	3.5 ± 1.0	.297
LPI	10.5 ± 6.3	8.0 ± 5.1	.404
LPC	8.5 ± 4.4	6.3 ± 4.9	.094
LPS	10.5 ± 4.8	6.2 ± 3.1	.008
RR	11.1 ± 4.6	6.8 ± 3.9	.005
RAS	11.8 ± 6.1	8.0 ± 5.1	.036
RAC	7.0 ± 3.1	7.4 ± 3.9	.753
RAI	8.5 ± 3.7	7.3 ± 5.8	.527
RB	4.6 ± 1.8	3.4 ± 0.6	.183
RPI	12.6 ± 5.9	6.8 ± 3.3	.001
RPC	9.0 ± 3.8	4.3 ± 1.0	<.001
RPS	9.6 ± 5.9	5.3 ± 3.0	.049
Average	8.2 ± 2.2	5.6 ± 2.0	.001

LR, roof segment of the left PV; LAS, anterior-superior segment of the left PV; LAC, anterior-carina of the left PV; LAI, anterior-inferior segment of the left PV; LB, bottom segment of the left PV; LPI, posterior-inferior segment of the left PV; LPC, posterior-carina of the left PV; LPS, posterior-superior of the left PV; RR, roof segment of the right PV; RAS, anterior-superior segment of the right PV; RAC, anterior-carina of the right PV; RAI, anterior-inferior segment of the right PV; RB, bottom segment of the right PV; RPI, posterior-inferior segment of the right PV; RPC, posterior-carina of the right PV; RPS, posterior-superior of the right PV.

3.4 | CK elevation after Ablation

The baseline CK value was comparable between the two groups (118 (89; 157) IU/L in the CB group vs 130 (86; 167) IU/L in the RF group, $P = .707$). The CK value was significantly elevated after the CB ablation, but not after the RF ablation (CK value in the CB group: 118 (89; 157) to 329 (257; 409) IU/L, $P < .001$; CK value in the RF group 130 (86; 167) to 123 (1106; 151) IU/L, $P = .670$) (Figure 5). No symptom of acute coronary syndrome, myocarditis, rhabdomyolysis, malignant hyperthermia, and malignant syndrome was documented in any patients. Therefore, the elevation of CK value after CB ablation could be caused by the massive cryothermal injury to the myocardium.

4 | DISCUSSION

4.1 | Main findings

As compared to the lesions after the RF ablation, the lesions after the CB ablation could be characterized as follows: 1) the overall lesion width was significantly wider; 2) the lesion gaps were significantly fewer at the LAS and RAI; and 3) the degree of myocardial injury was extremely higher.

4.2 | Ablation lesion width assessed by LGE-MRI

Although the lesions after RF ablation have been reported to be visualized by LGE-MRI in the previous studies, the difference in the LGE lesions between CB and RF ablation is still in debate.^{8,16}

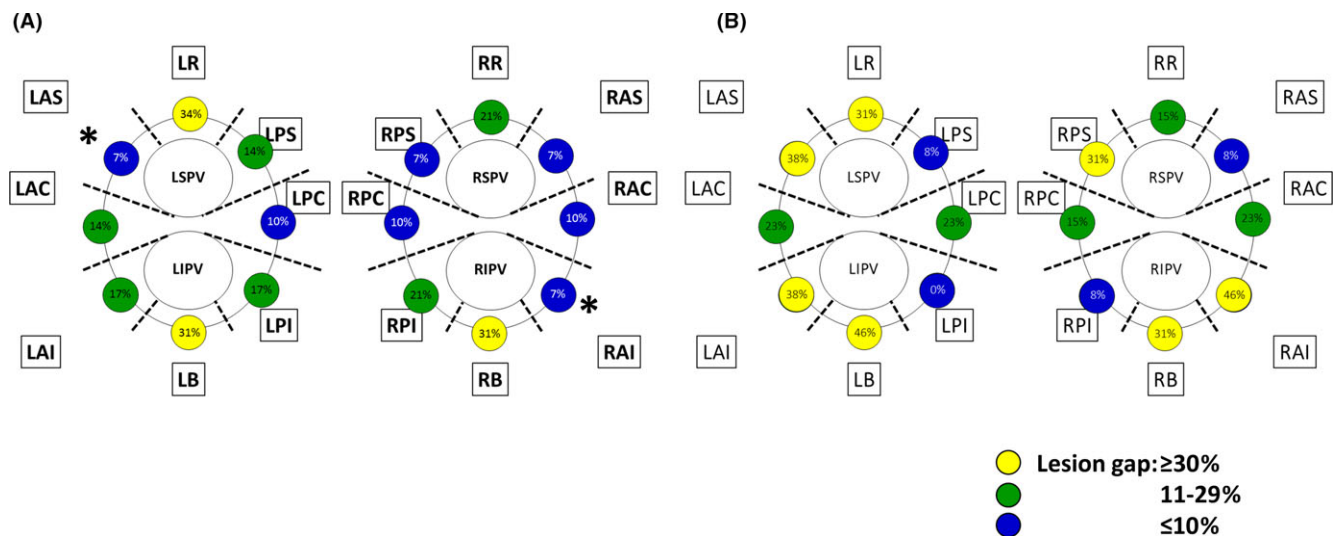


FIGURE 3 Comparison of the ablation lesion gap between the CB and RF groups. A, Lesion gap after CB ablation. B, Lesion gap after RF ablation. Numbers indicate the percentage of the segment with lesion gaps found in each segment. For each segment, 29 and 13 segments were analyzed in the CB and RF groups, respectively. Lesion gaps were significantly fewer at the anterior-superior segment of the left PV (LAS) and anterior-inferior segment of the right PV (RAI) in the CB group as compared to the RF group (LAS: 2 [7%] of 29 in CB group vs 5 [38%] of 13 in RF group, $P = .021$; RAI: 2 [7%] of 29 in CB group vs 6 [46%] of 13 in RF group, $P = .006$). Three segments with highly documented lesion gap were found in the CB group, while 7 segments in the RF group (the yellow circle). Please see the detail number and percentage of the lesion gap in the text. * Significantly different at $P < .05$

TABLE 3 Ablation lesion gap between the CB and RF groups

	CB group N = 29 Gap positive n, (%)	RF group N = 13 Gap positive n, (%)	P value
LR	10 (34)	4 (30)	.553
LAS	2 (7)	5 (39)	.021
LAC	4 (14)	3 (23)	.370
LAI	5 (17)	5 (39)	.136
LB	9 (31)	6 (46)	.273
LPI	5 (17)	0 (0)	.140
LPC	3 (10)	3 (23)	.262
LPS	4 (14)	1 (8)	.503
RR	6 (21)	2 (15)	.522
RAS	2 (34)	1 (7)	.682
RAC	3 (10)	3 (23)	.262
RAI	2 (7)	6 (46)	.006
RB	9 (31)	4 (31)	.640
RPI	6 (21)	1 (8)	.287
RPC	3 (10)	2 (15)	.497
RPS	5 (17)	4 (31)	.275

Please see Table 2 for the abbreviations.

Malcome-Lawes et al. reported that there was no difference in the amount of atrial and PV ostial scar by 3 months after CB or RF ablation procedures.¹⁶ They arbitrarily defined an LGE level of beyond 3-SD above the blood pool mean as atrial scar because LGE levels 3-SD above the blood pool mean are associated with significantly

lower bipolar and unipolar voltages compared to the preceding SD levels. Thus, the LGE intensity threshold and visualization method completely differed from ours. Although the area with an LGE threshold of above 3-SD might be associated with a low-voltage zone (LVZ), this might underestimate the ablation lesions. Furthermore, LA-voltage maps were created with the ablation catheter without contact sensing, which suggested that the LVZ might have been overestimated. Khurram et al. also reported that there was no difference in the PV antral LGE intensity between CB and RF ablation. However, the sample size was rather small (7 patients in the RF group and 5 in the CB group).⁸ The LGE-MRI acquisition protocol was consistent with other reports; however, the definition of the ablation lesion was still in debate. In our study, the definition of the ablation lesion was defined as an artificial LGE site with a signal intensity of $>2SD$ around the PV, which prioritized the sensitivity over the specificity for detecting the ablation lesion. Furthermore, animal study had reported that the maximum gap length with conduction block was 4 mm.¹⁵ According to the result, the lesion gap was defined as the site with non-LGE site of >4 mm, which prioritized the specificity over the sensitivity for detecting the lesion gap. Although the study result might have differed using the different threshold and definition of the ablation lesion and gap, we considered that a LGE threshold of $>2SD$ and gap length of >4 mm could contribute to improve the accuracy for detecting the actual ablation lesion and gaps. Our study demonstrated that the overall lesion width was significantly wider in the CB group than in the RF group. In the 1st procedure, touch-up RF ablation was performed in 6 (21%) of 29 CB group patients. The site of the touch-up RF ablation was the RIPV and LIPV in 4 and 3 patients, respectively. One patient

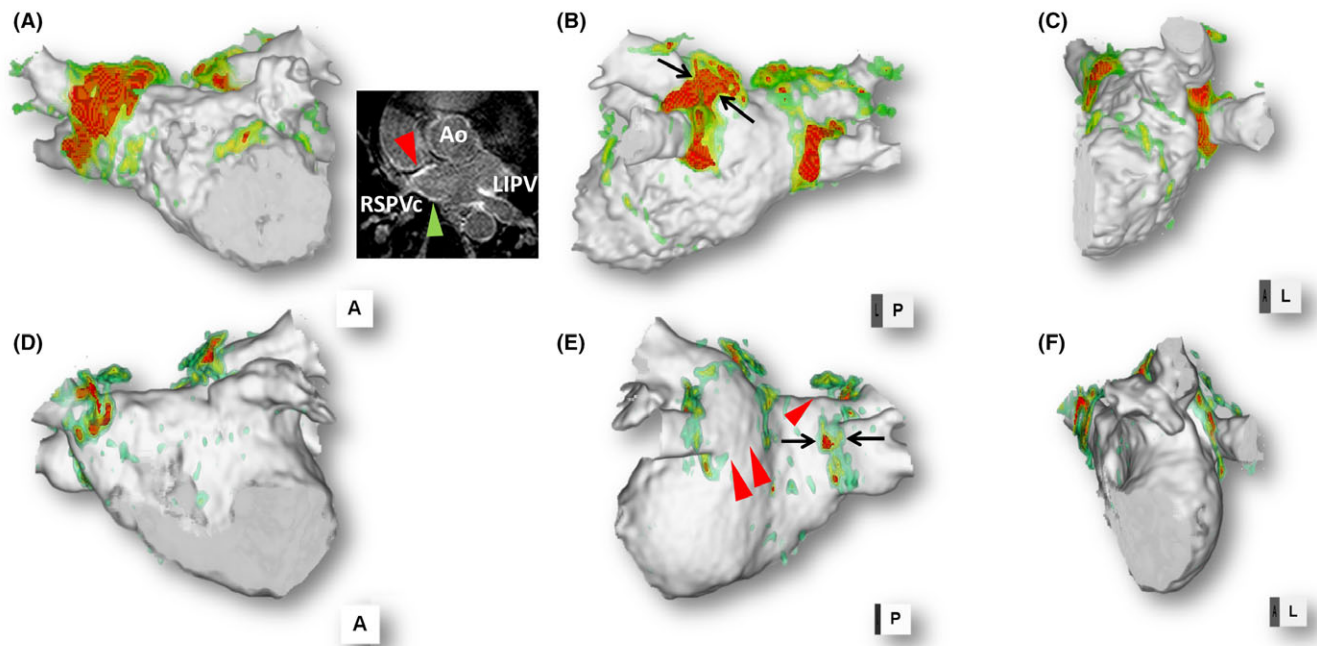


FIGURE 4 Representative cases after CB and RF ablation. A, B, and C: Representative case after a CB ablation. The right panel shows LA wall sliced after CB ablation. The black arrows indicate a lesion width at the posterior-superior segments of the left PV of 12 mm. D, E, and F: A representative case after RF ablation. The degree of intensity was categorized by color-coded scaling (green: >2SD; yellow: 3–4SD; red: >4SD). The LGE site categorized by the color-coded scaling “red” indicated the more massive lesion as compared to that by “yellow” and “green.” The red arrowhead on the LGE-MRI indicated the anterior wall of the RSPV where the gadolinium was extremely enhanced, which corresponded to the “red” area on the 3D reconstructed MRI, while the green arrowhead on the LGE-MRI indicated the posterior wall of the RSPV where the gadolinium was relatively enhanced, which corresponded to the “green” area on the 3D-reconstructed MRI. The black arrows indicate a lesion width at the posterior-inferior segment of the right PV of 5 mm. The red arrowheads indicate the lesion gaps at the posterior-inferior region of the left PV and posterior-superior segment of the right PV. Anterior-posterior view in the left panel (A, D), posterior-anterior view in the middle panel (B, E), and lateral view in the right panel (C, F). LA, left atrium; CB, cryoballoon; RF, radiofrequency; RSPV, right superior pulmonary vein; Ao, ascending aorta; LIPV, left inferior pulmonary vein

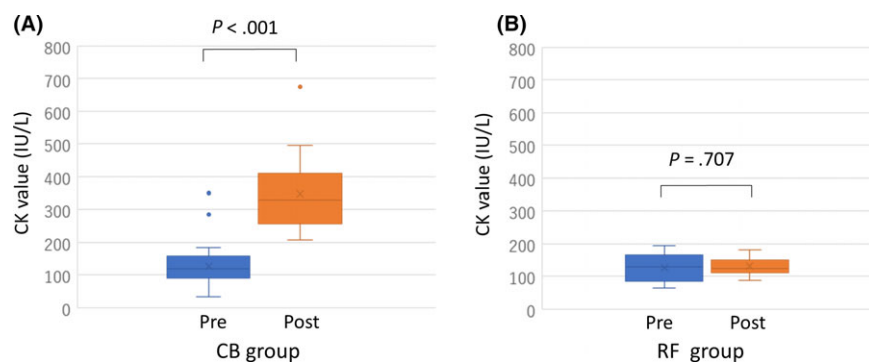


FIGURE 5 Postprocedural CK change. A, Postprocedural CK changes after the CB ablation. B, Postprocedural CK changes after the RF ablation. CK, Creatine kinase

required touch-up in both the RIPV and LIPV. Even though those 6 patients with touch-up RF ablation were excluded, the results were consistent and the impact was further strengthened.

The CK value after ablation was significantly more increased in the CB group than in the RF group. Casella et al. reported that the troponin I and CK-MB levels were significantly more increased after the CB ablation than after ablation with the other energy sources.¹⁷ This strongly indicated that the CB ablation could induce great

myocardial injury. We speculated that the cardiac injury after ablation was strongly associated with the ablation area.

4.3 | Ablation lesion gap assessed by LGE-MRI

Metzner et al. investigated the 2-year clinical outcome after CB ablation.¹⁸ Their patients underwent a repeat RF-based ablation due to recurrence of atrial tachyarrhythmia events. In the recurrence cases,

the reconnection sites were identified mainly at the inferior aspect of the inferior PVs and following the superior aspect of the superior PVs. They speculated that the CB tissue contact was not optimized at those regions, and the energy transfer was limited. Our study could clearly demonstrate that the lesion gaps after CB ablation were mainly located at the roof segments of the left PV (LR), bottom segment of the left PV (LB), and bottom segment of the right PV (RB). These findings were completely consistent with their results. However, conduction gaps were documented in 10 (59%) of 17 lesion gap sites in 5 patients who underwent 2nd AF procedure, while no conduction gap was documented at the site without lesion gap. This might support the accuracy of lesion gap for detecting conduction gap in the 2nd procedure. While the lesion gaps in the RF group were equally distributed in our study, those in the CB group were mainly documented at the LR, LB, and RB. Khurram et al. and Miyazaki et al. also reported that the left and right PV inferior aspects and superior segments tended to become the recurrence sites.^{8,19}

Peters et al. reported that a total of 35 AF patients underwent their first RF ablation and underwent an LGE MRI after 46 ± 28 days. The LIPV displayed the most circumferential LGEs (68%), followed by the RIPV (52%), RSPV (32%), and LSPV (31%).²⁰ Further, Parmer et al. studied 70 AF initial ablation patients who underwent an LGE MRI 3 months after the ablation. In their report, the LIPV also displayed the most circumferential LGEs (52.0%), followed by the LSPV (36.0%), RSPV (33.8%), and RIPV (27.9%).²¹ AF recurrences during the first year were reported to be associated with a lesser degree of PV and left atrial scarring on 3-dimensional LGE MRI. Furthermore, this finding was significant for RIPV scar. Focusing on the lesion width and gap founded at RAI, RB, and RPI in our study, the lesion width and gaps in the RF group were likely narrower and more frequent, respectively. The wide and continuous lesions around the RIPV might be one of the unique lesion characteristics after the CB ablation.

4.4 | Study limitations

Our study had several limitations. First, the sample size was small. Second, we performed no LGE MRI prior to the ablation procedure. Therefore, we could not discriminate between the ablation lesion and preexisting atrial fibrosis around the PV. This indicated that the ablation lesion around the PV might have been overestimated. Third, AF ablation with a conventional ablation catheter was applied in most of the patients with persistent AF, while most of the paroxysmal AF patients underwent AF ablation with a cryoballoon. Therefore, the patient characteristics, especially the LAD and AF type, significantly differed between the 2 groups. This issue might influence the width of the ablation lesion and number of lesion gaps. Fourth, touch-up RF ablation was performed in 6 of 29 CB group patients. The site of the touch-up RF ablation was the RIPV and LIPV in 4 and 3 patients, respectively. One patient required touch-up in both the RIPV and LIPV. Although single or double RF touch-up applications could achieve

PV-LA conduction block, the number of lesion gaps after the CB ablation might have been underestimated. Fifth, the duration from AF procedure to the MRI acquisition was relatively short as compared to the previous reports, which might overestimate the lesion extent and underestimate the lesion gap. However, the duration to the MRI acquisition was comparative between the CB and RF groups. As clinical research, this issue could be acceptable to accurately compare the difference of the lesion between two groups.

5 | CONCLUSIONS

The lesions after CB ablation could be characterized as being wider and more continuous than those after conventional RF ablation. To create durable and complete circular lesions around the PVs, adhesion to the roof of the LSPV and bottom of both PVs should be optimized during the CB ablation.

ACKNOWLEDGEMENTS

We would like to thank Mr. John Martin for his linguistic assistance.

CONFLICTS OF INTEREST

The Section of Arrhythmia is supported by an endowment from Medtronic JAPAN and St. Jude Medical JAPAN. The authors have reported that they have no relationship relevant to the contents of this manuscript to disclose.

ORCID

Kunihiko Kiuchi  <http://orcid.org/0000-0002-9305-4854>

Hiroshi Imada  <http://orcid.org/0000-0002-6884-9962>

REFERENCES

1. Chimura M, Kiuchi K, Okajima K, et al. Distribution of ventricular fibrosis associated with life threatening ventricular tachyarrhythmias in patients with nonischemic dilated cardiomyopathy. *J Cardiovasc Electrophysiol*. 2015;26:1239–46.
2. McGann CJ, Kholmovski EG, Oakes RS, et al. New magnetic resonance imaging-based method for defining the extent of left atrial wall injury after the ablation of atrial fibrillation. *J Am Coll Cardiol*. 2008;52:1263–71.
3. Marrouche NF, Wilber D, Hindricks G, et al. Association of atrial tissue fibrosis identified by delayed enhancement MRI and atrial fibrillation catheter ablation: the DECAAF study. *JAMA*. 2014;311:498–506.
4. Khurram IM, Habibi M, Gucuk Ipek E, et al. Left atrial LGE and arrhythmia recurrence following pulmonary vein isolation for paroxysmal and persistent AF. *JACC Cardiovasc Imaging*. 2016;9:142–8.
5. Peters DC, Wylie JV, Hauser TH, et al. Detection of pulmonary vein and left atrial scar after catheter ablation with three-dimensional navigator-gated delayed enhancement MR imaging: initial experience. *Radiology*. 2007;243:690–5.

6. Bisbal F, Guiu E, Cabanas-Grandio P, et al. MRI-guided approach to localize and ablate gaps in repeat AF ablation procedure. *JACC Cardiovasc Imaging*. 2014;7:653–63.
7. Kiuchi K, Fukuzawa K, Takaya T, et al. Homogenous and continuous lesion formation with cryoballoon ablation: delayed-enhancement magnetic resonance imaging analysis. *J Cardiovasc Electrophysiol*. 2016;27:1234–5.
8. Khurram IM, Catanzaro JN, Zimmerman S, et al. MRI evaluation of radiofrequency, cryothermal, and laser left atrial lesion formation in patients with atrial fibrillation. *Pacing Clin Electrophysiol*. 2015;38:1317–24.
9. Miyazaki S, Taniguchi H, Hachiya H, et al. Quantitative analysis of the isolation area during the chronic phase after a 28-mm second-generation cryoballoon ablation demarcated by high-resolution electroanatomic mapping. *Circ Arrhythm Electrophysiol*. 2016;9:e003879.
10. Kiuchi K, Kircher S, Watanabe N, et al. Quantitative analysis of isolation area and rhythm outcome in patients with paroxysmal atrial fibrillation after circumferential pulmonary vein antrum isolation using the pace-and-ablate technique. *Circ Arrhythm Electrophysiol*. 2012;5:667–75.
11. Kiuchi K, Okajima K, Shimane A, et al. Visualization of the radiofrequency lesion after pulmonary vein isolation using delayed enhancement magnetic resonance imaging fused with magnetic resonance angiography. *J Arrhythm*. 2015;31:152–8.
12. Kiuchi K, Okajima K, Shimane A, et al. Visualizing radiofrequency lesions using delayed-enhancement magnetic resonance imaging in patients with atrial fibrillation: a modification of the method used by the University of Utah group. *J Arrhythm*. 2015;31:71–5.
13. Kiuchi K, Okajima K, Shimane A, et al. Visualization of pulmonary vein-left atrium reconnection site on delayed-enhancement magnetic resonance imaging in the second atrial fibrillation catheter ablation. *Circ J*. 2014;78:2993–5.
14. McGann C, Akoum N, Patel A, et al. Atrial fibrillation ablation outcome is predicted by left atrial remodeling on MRI. *Circ Arrhythm Electrophysiol*. 2014;7:23–30.
15. Ranjan R, Kato R, Zviman MM, et al. Gaps in the ablation line as a potential cause of recovery from electrical isolation and their visualization using MRI. *Circ Arrhythm Electrophysiol*. 2011;4:279–86.
16. Malcolm-Lawes LC, Juli C, Karim R, et al. Automated analysis of atrial late gadolinium enhancement imaging that correlates with endocardial voltage and clinical outcomes: a 2-center study. *Heart Rhythm*. 2013;10:1184–91.
17. Casella M, Dello Russo A, Russo E, et al. Biomarkers of myocardial injury with different energy sources for atrial fibrillation catheter ablation. *Cardiol J*. 2014;21:516–23.
18. Metzner A, Heeger CH, Wohlmuth P, et al. Two-year outcome after pulmonary vein isolation using the second-generation 28-mm cryoballoon: lessons from the bonus freeze protocol. *Clin Res Cardiol*. 2016;105:72–8.
19. Miyazaki S, Taniguchi H, Hachiya H, et al. Clinical recurrence and electrical pulmonary vein reconnections after second-generation cryoballoon ablation. *Heart Rhythm*. 2016;13:1852–7.
20. Peters DC, Wylie JV, Hauser TH, et al. Recurrence of atrial fibrillation correlates with the extent of post-procedural late gadolinium enhancement: a pilot study. *JACC Cardiovasc Imaging*. 2009;2:308–16.
21. Parmar BR, Jarrett TR, Burgon NS, et al. Comparison of left atrial area marked ablated in electroanatomical maps with scar in MRI. *J Cardiovasc Electrophysiol*. 2014;25:457–63.

How to cite this article: Kurose J, Kiuchi K, Fukuzawa K, et al. The lesion characteristics assessed by LGE-MRI after the cryoballoon ablation and conventional radiofrequency ablation. *J Arrhythmia*. 2018;34:158–166. <https://doi.org/10.1002/joa3.12025>